Metallography, Microstructure, and Analysis (2018) 7:77–87
https://doi.org/10.1007/s13632-017-0412-3

TECHNICAL ARTICLE

Microstructure Evolution in Cast Al-Zn-Mg Alloys Processed by Equal Channel Angular Pressing

G. K. Manjunath[1] · K. Udaya Bhat[1] · G. V. Preetham Kumar[1]

Received: 24 October 2017 / Revised: 7 December 2017 / Accepted: 14 December 2017 / Published online: 26 December 2017

Abstract
In the present work, microstructure development and enhancement in the microhardness of Al-Zn-Mg alloys (with 5, 10, and 15% zinc) during equal channel angular pressing (ECAP) were investigated. Dendritic morphology was observed in the cast condition of all three alloys, and precipitates were situated along the inter-dendritic regions. After homogenization, precipitates in the inter-dendritic regions were uniformly distributed in the aluminum matrix and grain boundaries were developed. After 4 passes in route B_C, large reduction in the grain size was observed. X-ray diffractometry showed that $MgZn_2$ precipitate was developed in the ECAP-processed samples. Increase in the intensity of $MgZn_2$ peaks was observed when the quantity of zinc is increased in the material. Also, changes in the intensity of XRD peaks were observed in ECAP-processed samples due to shear deformation. After ECAP, substantial increase in the microhardness was perceived. After four passes, microhardness increased to 109, 67, and 58% from the initial condition in A1, A2, and A3 alloys, respectively. Also, improvement in the microhardness was also observed when the quantity of zinc is increased in the material.

Keywords XRD · Microstructure · Microhardness · Al-Zn-Mg alloy · ECAP

Introduction

Severe plastic deformation (SPD) methods have fascinated the interest of the researchers in the materials engineering domain due to several advantages compared to other processing techniques [1]. Numerous techniques are established for SPD processing of metallic materials. Among all available SPD methods, ECAP is innovative and effective technique to develop ultrafine-grained (UFG) materials in metals and alloys [2]. In 1981, Segal introduced the ECAP process [3], later on numerous used it on various materials. ECAP is a metal forming process, in which intense plastic strain is induced into the sample without altering the cross-sectional area, so the sample can be processed again and again to accomplish huge plastic strain [4]. The main advantage of ECAP processing is that ECAP processing results in high degree of grain refinement along with the formation of high-angle grain boundaries. Also, it is possible to develop required textures during ECAP by modifying the shear plane and direction during a multiple pressing sequence. The process can be easily scaled up for processing the bulk size samples. ECAP processing is characterized by several fundamental and experimental parameters which define the nature of the operation, and all these parameters play a critical role in determining the nature of the UFG structure obtained by ECAP. Also, these factors play a vital role in obtaining homogeneity in the microstructure, grain misorientation, crystallographic textures, and enhancement in the properties in the processed material. Major parameters involved in the ECAP processing are strain imposed in ECAP, the processing routes in ECAP, influence of the pressing temperature, and influence of the back pressure. Generally, ECAP-processed materials possess high dislocation densities which leads to much higher strength and hardness than the coarse-grained materials. Aluminum alloys are attractive materials in industrial uses due to their low density. Nowadays, the Al-Zn-Mg system is getting more attention because it is the strongest and hardest aluminum alloy, among all the aluminum alloys [5]. The Al-Zn-Mg alloys satisfy the major demand of industries in the development of lightweight materials having high strength and high

✉ G. K. Manjunath
manjugk2001@gmail.com

[1] Department of Metallurgical and Materials Engineering, National Institute of Technology Karnataka, Surathkal, Mangalore 575025, India

toughness characteristics. The main applications of these alloys are in military and aerospace applications [5].

It has been reported that ECAP processing enhances the mechanical properties in Al-5.7Zn-1.9Mg-1.5Cu alloy [6]. ECAP leads to a significant breaking of η' phase ($MgZn_2$) precipitates from the rodlike structure to the spherical particles, in spray-cast Al-11.5Zn-2.5Mg-0.9Cu alloy [7]. Crack initiation was studied through FEM analysis in ECAP-processed Al-4.13Zn-1.32Mg alloys by Ebrahimi et al. [8]. Suitability of ECAP for processing of cast Al-5Zn-1Mg alloy hollow samples at room temperature was studied by Valder et al. [9]. Texture evolution during ECAP of Al-11.5Zn-2.5Mg-0.9Cu alloy was studied by Wang et al. [10]. It was observed that the quantity of high-angle grain boundaries increased in Al-5.7Zn-2.2Mg-1.2Cu alloy with increase in the number of ECAP passes [11]. Superplastic elongation of more than 1000% was observed at higher temperature in the ECAP-processed samples of Al-11.5Zn-2.5Mg-0.9Cu alloy [12]. Purcek et al. studied the tensile behavior of Zn-12Al alloy processed by ECAP, and it was reported that strength of the alloy was increased with increase in the number of passes. It was mentioned that ECAP processing is an effective technique for improving the tensile ductility of binary Zn-Al alloys [13]. Aydin and Heyal studied the microstructural and mechanical properties of the ECAP-processed Al-20Zn alloy, and it was reported that ECAP processing leads to significant improvement in the tensile properties, impact toughness, and fatigue performance of the alloy [14]. Aydin studied the high-cycle fatigue behavior of Zn-60Al alloy processed by ECAP in route A and in route B_C, and it was reported that fatigue strength and fatigue life of the alloy were increased with ECAP processing. But it was also reported that higher fatigue strength was perceived in route B_C compared to route A [15]. The present research is inspired by the understanding that no efforts have been made in earlier investigations to study the effect of ECAP on a cast alloy composed of only aluminum, zinc, and magnesium with varying zinc content. Since Al-Zn-Mg alloys are promising lightweight materials, with possible applications in aerospace and automobile sectors, improving mechanical properties has been a focus for long time. In this research, cast Al-Zn-Mg alloys (with 5, 10, 15% zinc, and 2% fixed quantity of magnesium in all three alloys) were ECAP-processed to understand the effect of ECAP on the microstructure evolution and microhardness.

Materials and Experimental Procedure

Table 1 presents the nominal compositions of the alloys used in this studied in the present work. The details of sample preparation by casting were briefly discussed in our previous work [16]. Cast samples were homogenized at 480 °C for 20 h. For ECAP processing, samples from homogenized material were machined to Ø 16 mm and length 85 mm. Figure 1a shows the model of the ECAP die having $\Phi = 120°$ and $\Psi = 30°$, and Fig. 1b presents the orthographic view of the ECAP die used in the present study. The ECAP die was fabricated from hot die steel and heat-treated to 50 HRc. The die halves were hold together with the help of clamps, and these clamps were clamped with the help of bolts and nuts. Holes are provided in the ECAP die for placing heating coils to heat the die to the required processing temperature, and the same temperature is maintained during processing.

Table 1 Nominal composition of the alloys

Alloy designation	Al (wt.%)	Zn (wt.%)	Mg (wt.%)
A1	93	5	2
A2	88	10	2
A3	83	15	2

Figure 1c shows that the different processing routes have been developed based on the rotation of the specimen about the axis in between successive passes. These routes activate different slip systems during the processing, so that significant difference in microstructure is developed. Each processing route is defined by the combination of shear planes that undergo deformation during pressing. In route A, the sample is pressed repetitively without rotation between consecutive passes. In route B_A, the sample is rotated through 90° in the alternate directions between consecutive passes. In route B_C, the sample is rotated by 90° in the same sense (either clockwise or counterclockwise) between each consecutive passes. In route C, the sample is rotated by 180° between consecutive passes. The effectiveness of the ECAP routes, in grain refinement, is more in route B_C followed by routes C, A and B_A. It is observed that route A cannot result in a uniform effective strain distribution. Route B_C and route C can result in uniform effective strain distribution, but route B_C results in better distribution and uniformity of the effective strain in the billet compared to route C. Also, route B_C is the optimum processing route for attaining a homogeneous microstructure of equiaxed grains separated by high-angle grain boundaries [17]. Therefore, route B_C was adopted in the present study.

The literature on the ECAP indicates that the strength could be maximized by processing the material at low temperature. In this regard, all three alloys were attempted to process at minimum possible temperature. All three alloys were failed during ECAP processing at room temperature, 100 and 125 °C in the first pass itself. A1 alloy was successfully processed up to four number of passes in route B_C at 150 °C. But, A2 and A3 alloys were successfully processed in the first pass and they failed in the second pass in route B_C

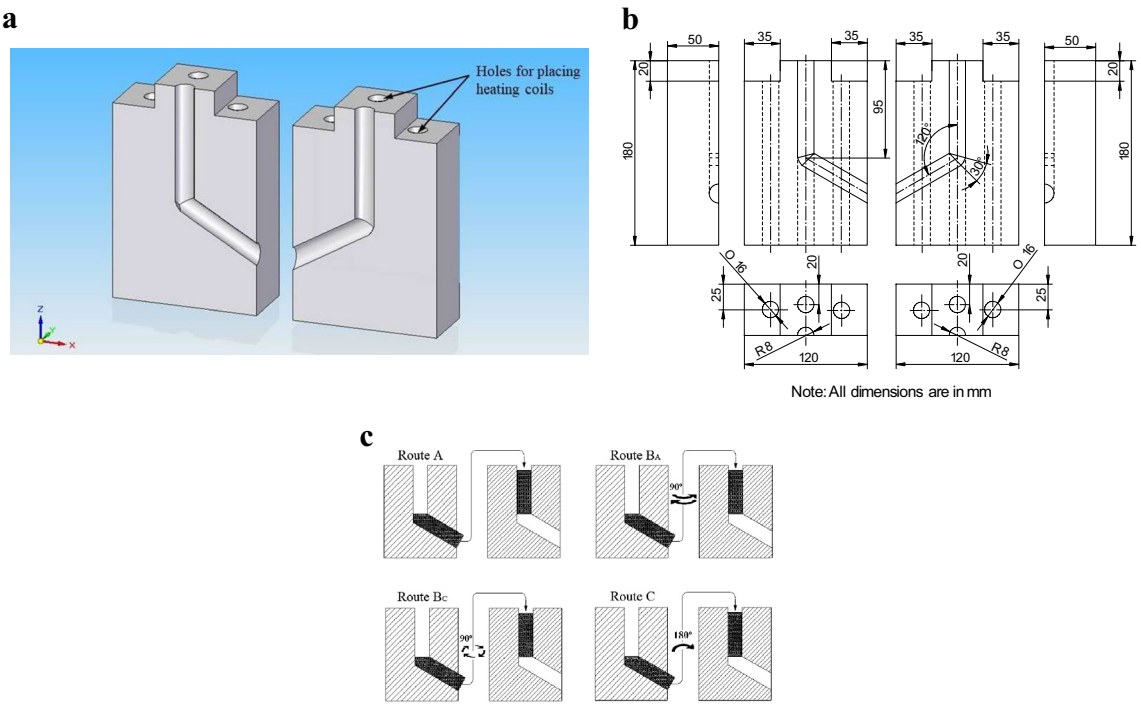

Fig. 1 (**a**) Model of the 120° ECAP die used in the present study. (**b**) Orthographic view of the ECAP die used in the present study. (**c**) The basic processing routes in ECAP

at 150 °C. A2 and A3 alloys were successfully processed up to four number of passes in route B_C at 200 °C. This was the lowest possible temperature at which the A2 and A3 alloys could be successfully ECAP-processed in route B_C, without cracking. Since the A1 alloy was successfully processed up to four number of passes in route B_C at 150 °C. It was easily processed at 200 °C up to four number of passes without any inconvenience. Therefore, all three alloys were successfully processed only at 200 °C. So, in the present study 200 °C was selected as the processing temperature. Processing was

Fig. 2 XRD plots of A1 alloy

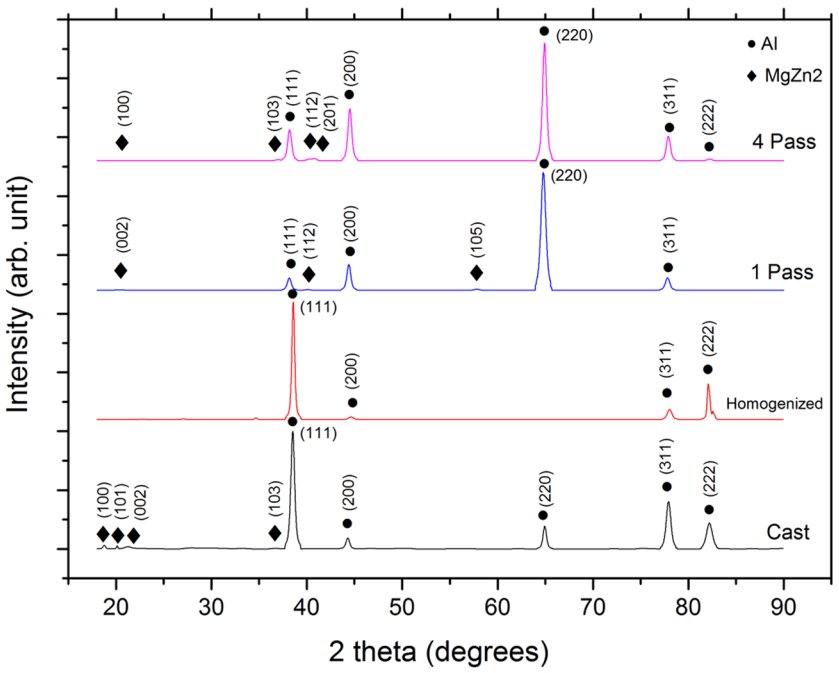

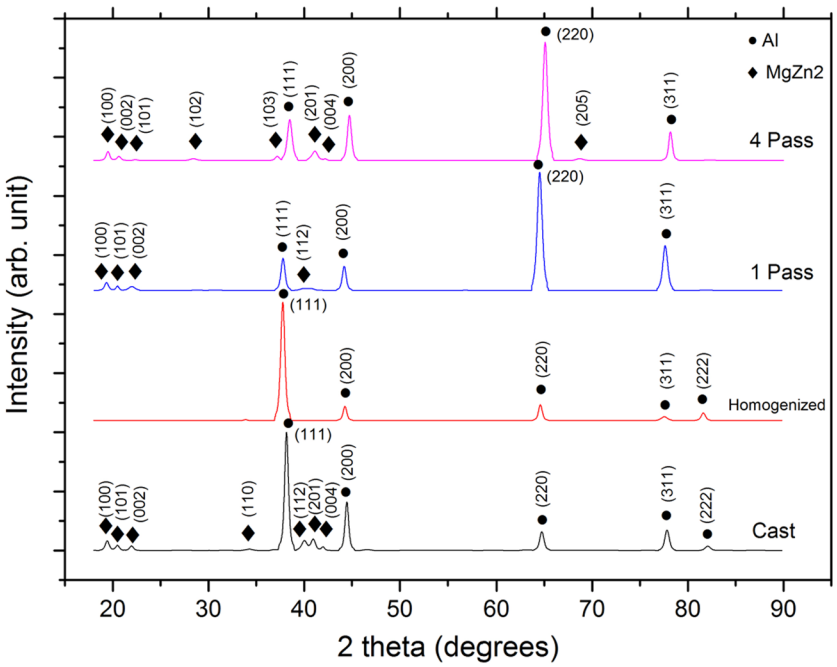

Fig. 3 XRD plots of A2 alloy

carried out in a 40 ton universal testing machine (UTM) at a pressing speed of 0.5 mm/s. Friction effect between the die and the sample was controlled by using molybdenum disulfide (MoS_2) lubricant.

To recognize the various phases existing in the material, X-ray diffractometer (XRD) analysis was conducted. The XRD studies were carried out with Cu-Kα radiation of 1.54 Å at 30 kV tube voltage and 20 mA current with a scanning speed of 1°/min. Microstructures of the unprocessed and processed samples were studied in scanning electron microscopy (SEM). For SEM study, cast and homogenized samples were sliced perpendicular to the ingot axis and ECAP-processed samples were sliced perpendicular to the processed direction. For microstructure study, samples were prepared by metallographic technique. Later, samples were etched with Keller's reagent. Grain size measurements were carried out in linear interception method. To measure the microhardness, center portion of the processed sample was

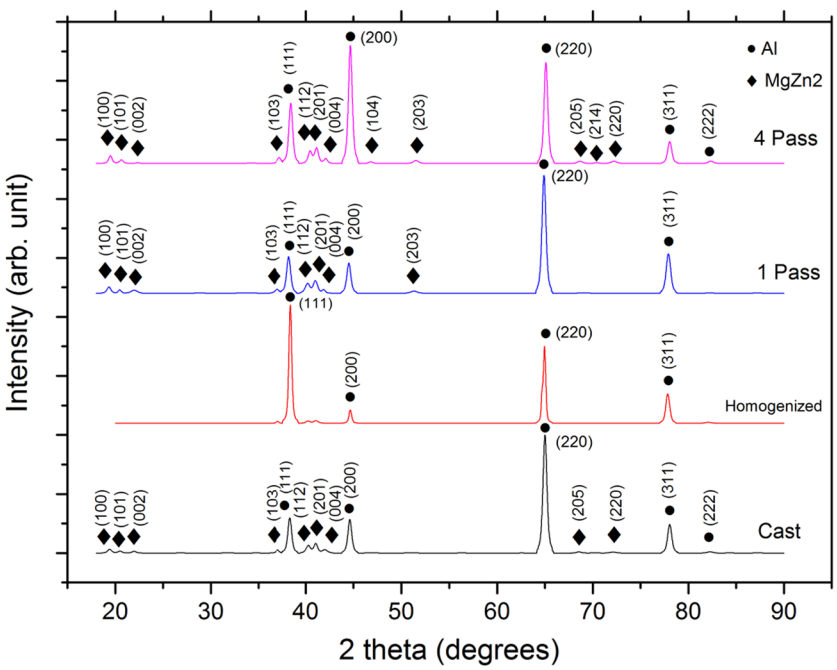

Fig. 4 XRD plots of A3 alloy

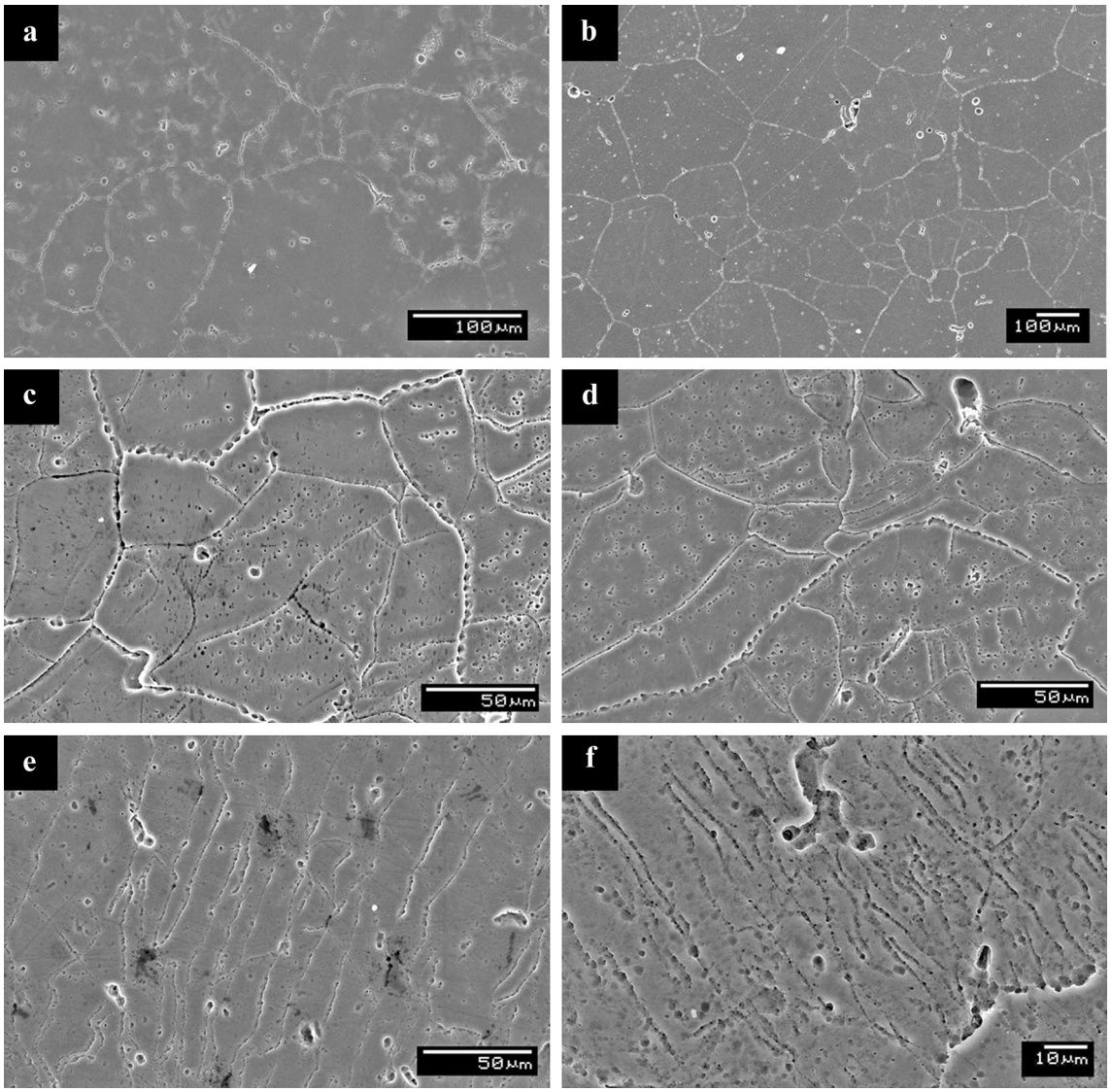

Fig. 5 SEM micrographs of A1 alloy (**a**) cast, (**b**) homogenized, (**c**) 1 pass, (**d**) 2 pass, (**e**) 3 pass, and (**f**) 4 pass

selected and hardness was measured perpendicular to the processing direction. Vickers microhardness, Hv, was determined at load = 50 gm and dwell time = 15 s. Totally, 12 measurements were taken randomly on the surface of the sample, and the average value was taken into consideration by eliminating the higher and lower values and averaging the remaining 10 measurements.

Results

XRD Analysis

XRD data for phase identification of A1, A2, and A3 alloy are shown in Figs. 2, 3, and 4, respectively. In cast condition, all 3 alloys exhibited peaks for aluminum and other phases. Peaks at 20° correspond to Guinier–Preston (GP) zones. Peaks at 40°–50° correspond to intermetallic hexagonal η' phase, and lattice parameter of these peaks is slightly bigger than η phase [18, 19]. After the homogenization, only aluminum peaks were observed, and these confirms that after homogenization precipitates segregated along the inter-dendritic regions were uniformly dissolved in the aluminum matrix, even in higher zinc content alloys. After first pass, the precipitates growth was observed in the alloy, because the dislocations provide space for the growth of the precipitates [18]. Very few precipitates were developed after first pass, and these were identified as GP zones and metastable η' phase. Increasing the ECAP passes, η' peaks move toward the η phase indicating the transformation of η' phase to stable η phase [18]. The formation of η' phase is shaped in the initial phase of first pass at 200 °C, and

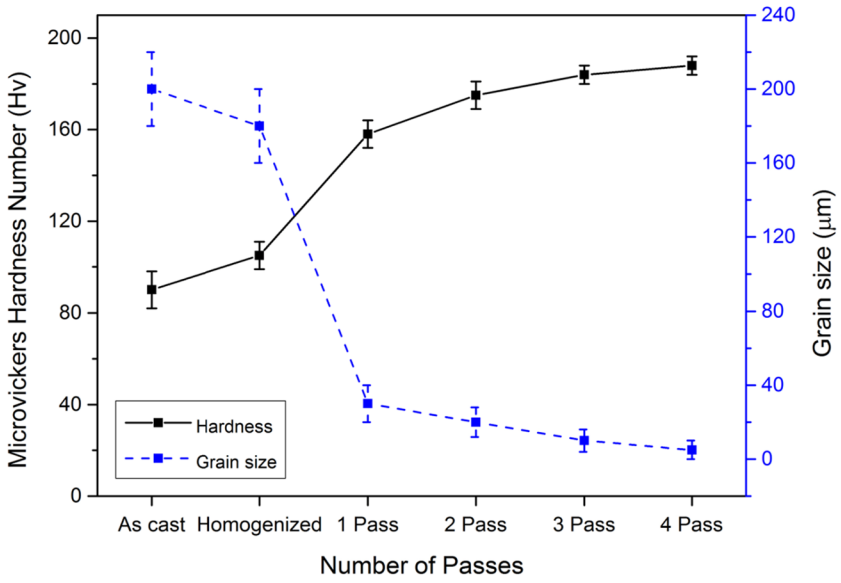

Fig. 6 Variation of microhardness and grain size of A1 alloy with ECAP passes

shearing of this phase takes place by the dislocations developed in the further passes. This leads to the development of small-size spherical shape η phase ($MgZn_2$) during ECAP at 200 °C [20]. The intensity of the precipitates increased with increase in the ECAP passes. After the fourth pass, stable η ($MgZn_2$) phase formed [18].

In cast and homogenized conditions, all three alloys exhibited strong (111) peaks. After first pass, the intensity of (111) peaks was reduced. This is owed to the grain refinement and texture weakening after the first pass. Even though the intensity of (111) plane increased after four passes, comparatively it is lesser than that in the as-cast condition. After ECAP processing, intensity of (200) reflection of aluminum is bigger than remaining peaks of aluminum, thereby representing the occurrence of a strong texture in the aluminum matrix after ECAP processing. From the XRD peaks, it was perceived that the intensity of $MgZn_2$ peaks increased with increasing when the zinc quantity is increased in the alloy. This confirms that when the zinc quantity in the alloy is increased, the amount of $MgZn_2$ precipitate in the alloy also increases.

Microstructural Analysis and Hardness

Figure 5 shows the SEM micrographs of A1 alloy in different conditions. Figure 5a shows that the microstructure of the cast alloy exhibits the characteristic feature of solidification structure composed of dendrites in the size 200 ± 20 μm. Also, precipitates were located along the inter-dendritic regions. These precipitates were recognized as η' phase ($MgZn_2$) precipitates [21]. After homogenization, the precipitates which were initially segregated along the inter-dendritic regions were uniformly distributed in the aluminum matrix and grain boundaries were developed, as shown in Fig. 5b. Dendritic structures present in the cast structure were completely disappeared after homogenization. In the homogenized condition, grains in the size 180 ± 20 μm were observed. In first pass, grain structure was significantly refined and sub-grain boundaries were developed inside the grains. Also, a few elongated grains were also observed as shown in Fig. 5c. A grain size of 30 ± 10 μm was observed, and the precipitates were developed near the grain boundaries. Figure 5d displays the microstructure of the alloy after second pass. The shape of the grain in this condition is similar to those observed in the alloy after first pass, and a grain size of 20 ± 8 μm was observed. After the third pass, shear bands were developed within the grains and sub-grains as shown in Fig. 5e and width of these deformation bands was 10 ± 6 μm. Figure 5f shows the microstructure of the alloy after fourth pass. In this condition, more number of shear bands was perceived and lateral dimension (width) of these bands was 5 ± 3 μm. Figure 6 illustrates the variation of microhardness and grain size of A1 alloy in different conditions. It is observed that microhardness of the alloy increases with decrease in the grain size. The microhardness in the cast condition was 90 Hv; after homogenization, it is increased to 105 Hv. Noticeable improvements in the microhardness of the alloy were observed after ECAP processing. The microhardness of the alloy was improved to 158 Hv in first pass, 175 Hv in second pass, 184 Hv in third pass, and 188 Hv in fourth pass. After homogenization, the microhardness was improved by 17%. After first and second passes, microhardness was improved by 76 and 94%, respectively, from the initial cast condition. After third and fourth passes, the microhardness was improved by 104 and 109%, respectively, from the initial condition.

Figure 7 illustrates the SEM micrographs of A2 alloy in different conditions. Figure 7a shows the microstructure of

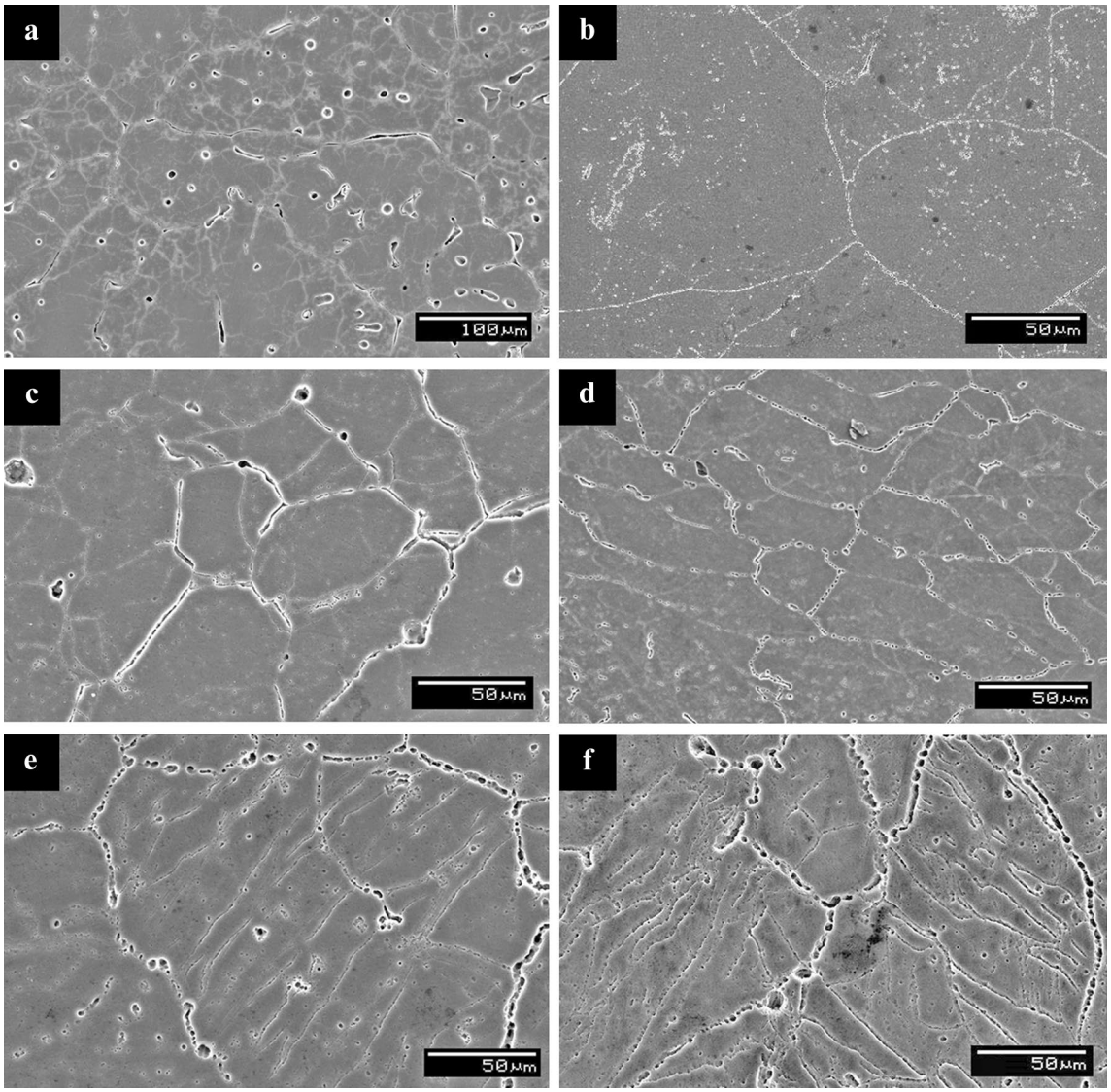

Fig. 7 SEM micrographs of A2 alloy (**a**) cast, (**b**) homogenized, (**c**) 1 pass, (**d**) 2 pass, (**e**) 3 pass, and (**f**) 4 pass

the cast alloy; similar to A1 alloy, the microstructure of A2 alloy in cast condition is constructed with dendritic morphology and precipitates were sited in the inter-dendritic regions. These precipitates were recognized as η' phase ($MgZn_2$) precipitates [21]. Dendrites were in the size of 280 ± 40 µm. It was observed that compared to A1 alloy the quantity of precipitates developed is more in A2 alloy in the cast condition. After homogenization treatment, precipitates segregated along the inter-dendritic regions were uniformly distributed in the aluminum matrix and grain boundaries were developed as shown in Fig. 7b. In the homogenized condition, grains in the size 260 ± 20 µm were observed. After first pass, grain structure was significantly refined as shown in Fig. 7c. In this condition, sub-grain boundaries were developed inside the grains and grain size of 75 ± 10 µm was observed. Also, precipitates were developed near the grain boundaries. Figure 7d shows the microstructure of the alloy after second pass. In this condition, a grain size of 40 ± 8 µm was observed. After the third pass, deformation bands were developed within the grains and sub-grains as shown in Fig. 7e, and width of these shear bands was 20 ± 7 µm. After fourth pass, more number of deformation bands were perceived and width (lateral dimension) of these bands was 8 ± 5 µm as illustrated in Fig. 7f. Figure 8 shows the variation of the microhardness and grain size of A2 alloy in different conditions. The microhardness in the cast condition was 144 Hv; after homogenization, it is increased to 155 Hv. The microhardness of the alloy was improved to 204 Hv in first pass, 223 Hv in second pass, 232 Hv in third pass, and 240 Hv in fourth pass. After homogenization treatment, the microhardness was improved by 8%. After first and the second passes, the microhardness was improved by 42 and

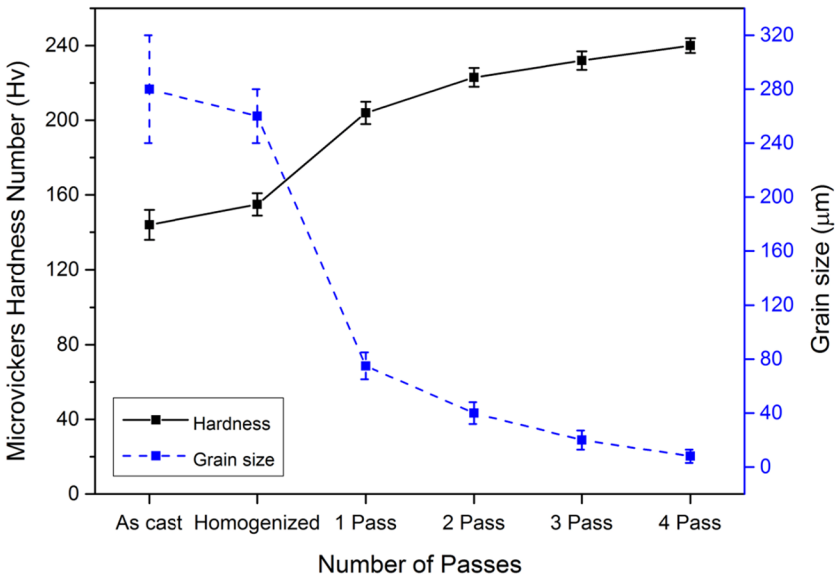

Fig. 8 Variation of microhardness and grain size of A2 alloy with ECAP passes

55%, respectively, from the cast condition. After third and the fourth passes, microhardness was improved by 61 and 67%, respectively, from the initial condition.

Figure 9 shows the SEM micrographs of A3 alloy in different conditions. Figure 9a illustrates the microstructure of the alloy in the cast condition. The microstructure is similar to those perceived in A1 and A2 alloys. The microstructure is built with dendritic structure, and precipitates were sited along the inter-dendritic regions. These precipitates were recognized as η' phase ($MgZn_2$) precipitates [21]. Dendrites were in the size of 200 ± 20 μm. It was observed that compared to A1 and A2 alloys the quantity of precipitates developed is more in A3 alloy, in the cast condition. After homogenization, precipitates which were initially segregated along the inter-dendritic regions were uniformly distributed in the aluminum matrix and grain boundaries were developed as shown in Fig. 9b. In the homogenized condition, grains in the size 180 ± 18 μm were observed. After first pass, grain structure was significantly refined as shown in Fig. 9c. In this condition, sub-grain boundaries were developed inside the grains and grain size of 50 ± 15 μm was observed. The microstructure of the alloy after the second pass is shown in Fig. 9d. In this condition, grains are similar to those observed in the alloy after first pass; sub-grains in the size of 25 ± 10 μm were perceived. After the third pass, sub-grains in the size of 15 ± 5 μm were observed as shown in Fig. 9e. The microstructure of the alloy after fourth pass is shown in Fig. 9f. In this condition, the sub-grains in the size of 10 ± 5 μm were observed. Figure 10 illustrates the variation of the microhardness and grain size of A3 alloy with different conditions. The microhardness in the cast condition was 173 Hv; after homogenization, it was improved to 189 Hv. The microhardness of the alloy was improved to 239 Hv in first pass, 261 Hv in second pass, 274 Hv in third and fourth passes, respectively. After homogenization treatment, 10% improvement in the microhardness was observed. After first and second passes, the microhardness was improved by 38 and 51%, respectively, from the initial condition. After third pass, microhardness was improved by 58% from the as-cast condition. It was observed that after the fourth pass the microhardness value was unchanged from that of the third pass.

Discussion

Higher strengthening can be achieved in ECAP processing compared to other conventional processing techniques. This strengthening may be credited to various mechanisms like grain refinement strengthening, dislocation strengthening, solid solution strengthening, and precipitation strengthening. The Al-Zn-Mg alloys form precipitates in the conventional sequence leading from the solid solution to GP zones followed by metastable precipitate η' and by the equilibrium phase η. The equilibrium phase η ($MgZn_2$) has the hexagonal structure [22]. GP zones are developed in the temperature range from room temperature up to 120 °C [22]. GP zones are coherent with the aluminum matrix. While η' phase ($MgZn_2$) is a metastable hexagonal phase ($a = 0.496$ nm, $c = 1.403$ nm), they are semi-coherent with the aluminum matrix. The equilibrium phase, η ($MgZn_2$), has the hexagonal structure ($a = 0.5221$ nm, $c = 0.8567$ nm); it is incoherent with the aluminum matrix. It was also perceived that ECAP process promotes precipitation kinetics [20]. Also, shear deformation occurring during the ECAP processing is expected to change the texture from the initial condition. Chowdhury et al. deduced that, after the first pass, the

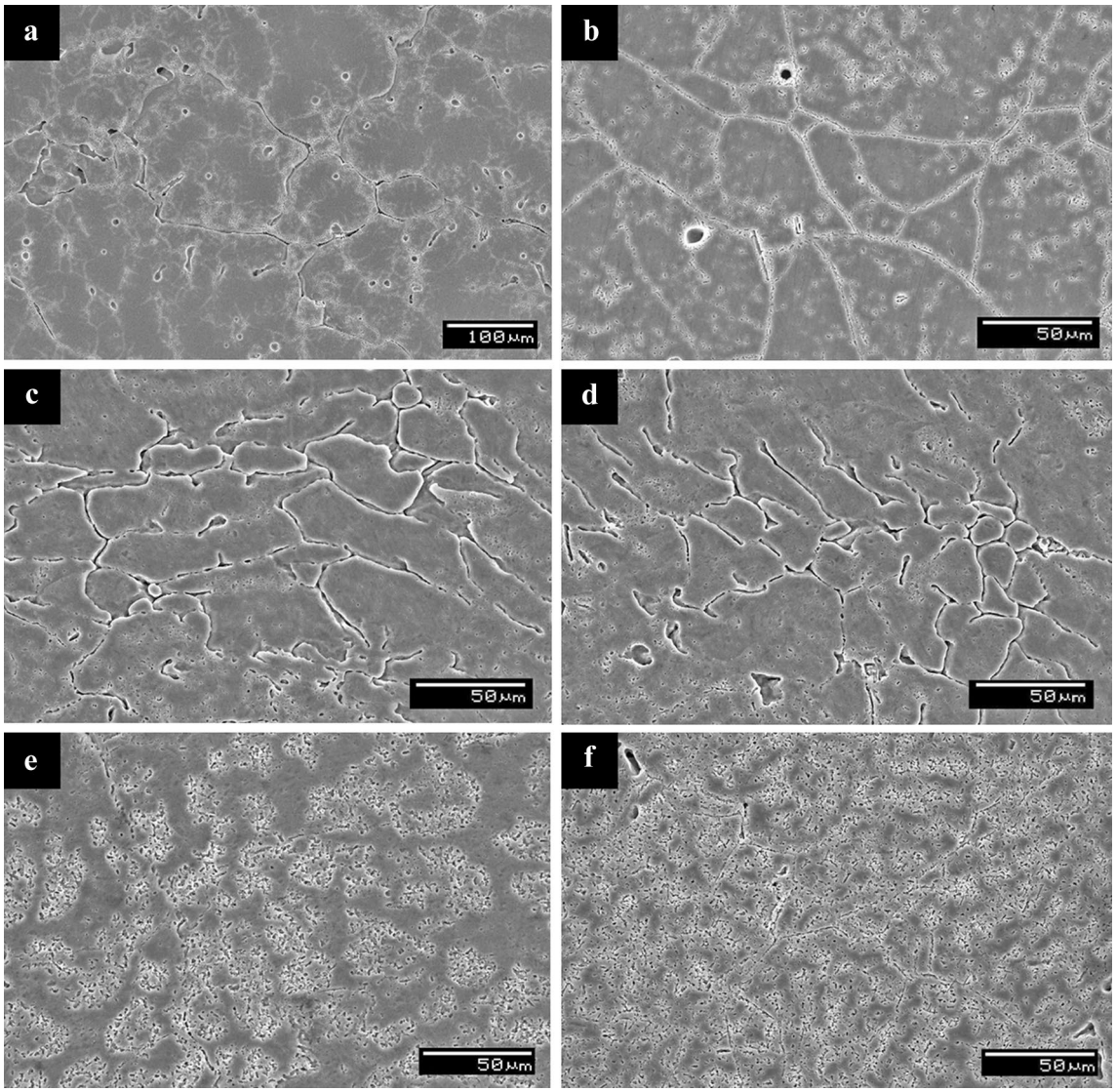

Fig. 9 SEM micrographs of A3 alloy (**a**) cast, (**b**) homogenized, (**c**) 1 pass, (**d**) 2 pass, (**e**) 3 pass, and (**f**) 4 pass

texture was deviated from the initial condition, and after the six passes, texture gradually moves toward the initial condition [23]. This may be the reason for change in the intensity of (111) and (200) peaks after ECAP processing. It was also observed that changes in texture occur due to changes in dislocation density taking place during ECAP processing [20]. It may be noted that there is an interaction between the shear plane and the texture formed during ECAP [24].

The results from the present investigation confirm that ECAP processing leads to substantial grain refinement in the alloy. It may be noted that, in route B_C deformation restores the equiaxed structure in each plane after every four consecutive passes and deformation will take place in all three planes. Also, processing in route B_C gives shearing over larger angular ranges by comparison with other processing routes [24]. It is observed that, compared to A1 alloy, quantity of precipitates developed is more in A2 alloy after ECAP. Likewise, compared to A1 and A2 alloys the quantity of precipitates developed is more in A3 alloy after ECAP. It is attributed to the increase in the quantity of zinc content in the alloy. The tendency for precipitate nucleation and growth was much more when the zinc content is increased in the alloy. In all three alloys, equiaxed and homogeneous microstructure was observed in third and fourth passes. This may be attributed to the dynamic recrystallization happened in ECAP processing at higher temperature and static recrystallization happened during initial heating of the sample.

In all three alloys, significant increase in the microhardness was observed after ECAP processing. The increase in microhardness is due to reduction in the grain size to submicrometer range, strain, or work hardening of the alloys owing to high dislocation density developed during ECAP

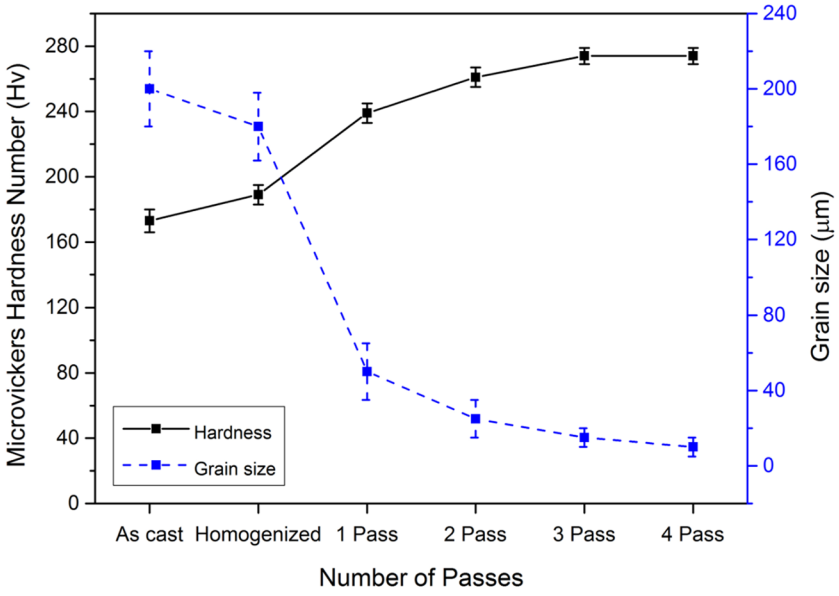

Fig. 10 Variation of microhardness and grain size of A3 alloy with ECAP passes

processing and development of finer precipitates which is homogenously distributed in the alloy [18]. Strength of the material is improved by dislocation network formed during ECAP processing. Since the moving dislocations are enforced to slice the regions of high dislocation density. With increasing in the amount of strain, group of tangles gradually grows into sub-grain boundaries. With increase in the plastic strain, disorientation and sharpening of these sub-grains take place with respect to the neighboring sub-grains [25]. After first pass, large improvement in the hardness was perceived compared to remaining passes. Similar trend was also perceived by Kim et al. in Al 7075 alloy processed by ECAP [26]. The strength and hardness Al 7075 alloy was increased in ECAP processing, due to the presence of η' ($MgZn_2$) phase precipitates [5]. Possibly, these precipitates are nucleated at the dislocation and other defects created during ECAP passes. The incremental defect density is more during initial ECAP passes compared to subsequent ECAP passes. Due to this, increase in the mechanical properties is much more during initial ECAP passes. Also, after the second pass there is no significant increase in the microhardness values.

It was also perceived that the microhardness increases when the quantity of zinc content in the alloy is increased. From XRD analysis, it was concluded that if the zinc quantity is increased in the alloy, the quantity of $MgZn_2$ precipitate in the alloy increases. So the amount of precipitates present in A2 alloy compared to A1 alloy is more. Similarly, the amount of precipitates present in A3 alloy compared to A1 and A2 alloy is more. If the quantity of precipitate increases in the alloy, hardness of the alloy improved. This might be the reason for improvement in the hardness of the material when quantity of zinc content is increased in the alloy. So, the combination of increase in the precipitate along with the increase in the defect density is attributed to high mechanical properties of ECAP-processed A3 alloy compared to other two alloys. The high density of dislocations generated during ECAP plays an important role for precipitation evolution.

Table 2 presents the ultimate tensile strength (UTS) of the alloys in various conditions. It was observed that significant increase in the UTS of the alloys was observed after ECAP processing. From the microstructural analysis, it was perceived that grain size of the alloys was decreased with the ECAP passes. According to the Hall–Petch equation, decreasing the grain size will increase the strength and hardness of the material. Along with grain refinement, increase in dislocation density and work hardening after ECAP processing are the main reasons for increase in the UTS of the alloys. After four passes, UTS of the alloys increased to 122, 153, and 139% from the initial condition in A1, A2, and A3 alloys, respectively. Detailed investigations on the tensile properties and tensile fracture characteristics of these alloys were presented in our earlier wok [16]. It was observed that similar to hardness the UTS of the alloy increased when quantity of zinc content is increased in the alloy.

Table 2 Ultimate tensile strength of the alloys in various conditions

	Ultimate tensile strength (MPa)		
	A1 alloy	A2 alloy	A3 alloy
Cast	120 ± 12	140 ± 10	166 ± 12
Homogenized	132 ± 12	156 ± 10	180 ± 11
First pass	218 ± 11	280 ± 9	340 ± 9
Second pass	244 ± 9	318 ± 9	372 ± 7
Third pass	256 ± 7	342 ± 8	392 ± 6
Fourth pass	266 ± 6	355 ± 6	396 ± 6

Conclusions

In the present research, microstructure evolution in cast Al-Zn-Mg alloys (5, 10 and 15% zinc) processed by ECAP was studied. The main conclusions of this research are as follows.

- The intensity of (111) and (200) reflections was changed after ECAP processing due to the shear deformation. The intensity of $MgZn_2$ precipitates in the alloy is increased when the quantity of zinc content in the alloy is increased. Dislocations generated during ECAP processing act as nucleation sites for the growth of precipitates.
- Microstructural investigations indicate that significant grain refinement was achieved after ECAP. Initially, dendrites of size 200 ± 20, 280 ± 40, and 200 ± 20 μm were perceived in the cast condition in A1, A2, and A3 alloys, respectively. After 4 passes, grain size was reduced to 5 ± 3, 8 ± 5, and 10 ± 5 μm in A1, A2, and A3 alloys, respectively.
- After ECAP, considerable increase in the microhardness was perceived. After four passes, the microhardness was improved to 188 Hv (94% increase), 240 Hv (67% increase), and 274 Hv (58% increase) from the initial condition in A1, A2, and A3 alloys, respectively. Similar to hardness, the UTS of the alloy also increased after ECAP processing. Also, microhardness and UTS of the alloy increase when the quantity of zinc content in the alloy is increased.

References

1. R.Z. Valiev, R.K. Islamgaliev, I.V. Alexandrov, Bulk nanostructured materials from severe plastic deformation. Prog. Mater Sci. **45**(2), 103–189 (2000)
2. R.Z. Valiev, T.G. Langdon, Principles of equal-channel angular pressing as a processing tool for grain refinement. Prog. Mater Sci. **51**(7), 881–981 (2006)
3. V.M. Segal, V.I. Raznikov, A.E. Drobyshewsky, V.I. Kopylov, Plastic working of metals by simple shear. Russ. Metall. **1**, 99–106 (1981)
4. Y.T. Zehetbauer, M.J. Zhu, *Bulk Nanostructured Materials* (Wiley-VCH, Weinheim, 2009)
5. M.H. Shaeri, M.T. Salehi, S.H. Seyyedein, M.R. Abutalebi, J.K. Park, Microstructure and mechanical properties of Al-7075 alloy processed by equal channel angular pressing combined with aging treatment. Mater. Des. **57**, 250–257 (2014)
6. Y.H. Zhao, X.Z. Liao, Y.T. Zhu, R.Z. Valiev, Enhanced mechanical properties in ultrafine grained 7075 Al alloy. J. Mater. Res. **20**(2), 288–291 (2005)
7. M.J. Starink, N. Gao, M. Furukawa, Z. Horita, C. Xu, T.G. Langdon, Microstructural developments in a spray-cast Al-7034 alloy processed by equal-channel angular pressing. Rev. Adv. Mater. Sci. **7**(1), 1–12 (2004)
8. M. Ebrahimi, S. Attarilar, C. Gode, F. Djavanroodi, Damage prediction of 7025 aluminium alloy during equal-channel angular pressing. Int. J. Miner. Metall. Mater. **21**(10), 990–998 (2014)
9. J. Valder, M. Rijesh, A.O. Surendranathan, Failure analysis of cast tubular specimens of Al-5Zn-Mg while processing at room temperature by equal channel angular pressing (ECAP). J. Fail. Anal. Prev. **14**(5), 690–695 (2014)
10. S.C. Wang, M.J. Starink, N. Gao, X.G. Qiao, C. Xu, T.G. Langdon, Texture evolution by shear on two planes during ECAP of a high-strength aluminium alloy. Acta Mater. **56**(15), 3800–3809 (2008)
11. C.M. Cepeda-Jimenez, J.M. Garcia-Infanta, O.A. Ruano, F. Carreno, Mechanical properties at room temperature of an Al-Zn-Mg-Cu alloy processed by equal channel angular pressing. J. Alloys Compd. **509**(35), 8649–86560 (2011)
12. C. Xu, T.G. Langdon, Creep and superplasticity in a spray-cast aluminium alloy processed by ECA pressing. Mater. Sci. Eng. A **410–411**, 398–401 (2005)
13. G. Purcek, M. Aydin, O. Saray, T. Kucukomeroglu, Enhancement of tensile ductility of severe plastically deformed two-phase Zn-12Al alloy by equal channel angular extrusion. Mater. Sci. Forum **633–634**, 437–447 (2010)
14. M. Aydin, Y. Heyal, Effect of equal channel angular pressing on microstructural and mechanical properties of as cast Al-20 wt%Zn alloy. Mater. Sci. Technol. **29**(6), 679–688 (2013)
15. M. Aydin, High-cycle fatigue behaviour of severe plastically deformed binary Zn-60Al alloy by equal-channel angular extrusion. J. Mater. Process. Technol. **212**(8), 1780–1789 (2012)
16. G.K. Manjunath, G.V. Preetham Kumar, K. Udaya Bhat, Tensile properties and tensile fracture characteristics of cast Al-Zn-Mg alloys processed by equal channel angular pressing. Trans. Indian Inst. Met. **70**(3), 833–842 (2017)
17. K. Nakashima, Z. Horita, M. Nemoto, T.G. Langdon, Development of a multi-pass facility for equal-channel angular processing to high total strains. Mater. Sci. Eng. A **281**(1–2), 82–87 (2000)
18. K.R. Cardoso, D.N. Travessa, W.J. Botta, A.M. Jorge Jr., High strength AA7050 Al alloy processed by ECAP: microstructure and mechanical properties. Mater. Sci. Eng. A **528**(18), 5804–5811 (2011)
19. Y.H. Zhao, X.Z. Liao, Z. Jin, R.Z. Valiev, Y.T. Zhu, Microstructures and mechanical properties of ultrafine grained 7075 Al alloy processed by ECAP and their evolutions during annealing. Acta Mater. **52**(15), 4589–4599 (2004)
20. J. Gubicza, I. Schiller, N.Q. Chinh, J. Illy, Z. Horita, T.G. Langdon, The effect of severe plastic deformation on precipitation in supersaturated Al-Zn-Mg alloys. Mater. Sci. Eng. A **460–461**, 77–85 (2007)
21. S. Zhang, W. Hu, R. Berghammer, G. Gottstein, Microstructure evolution and deformation behaviour of ultrafine-grained Al-Zn-Mg alloys with fine η′ precipitates. Acta Mater. **58**(20), 6695–6705 (2010)
22. N.Q. Chinh, J. Gubicza, T. Czeppe, J. Lendvai, C. Xu, R.Z. Valiev, T.G. Langdon, Developing a strategy for the processing of age-hardenable alloys by ECAP at room temperature. Mater. Sci. Eng. A **516**(1–2), 248–252 (2009)
23. S.G. Chowdhury, C. Xu, T.G. Langdon, Texture evolution in an aluminium alloy processed by ECAP with concurrent precipitate fragmentation. Mater. Sci. Eng. A **473**(1–2), 219–225 (2008)
24. M. Furukawa, Z. Horita, T.G. Langdon, Factors influencing the shearing patterns in equal-channel angular pressing. Mater. Sci. Eng. A **332**(1–2), 97–109 (2002)
25. L.J. Zheng, C.Q. Chen, T.T. Zhou, P.Y. Liu, M.G. Zeng, Structure and properties of ultrafine-grained Al-Zn-Mg-Cu and Al-Cu-Mg-Mn alloys fabricated by ECA pressing combined with thermal treatment. Mater. Charact. **49**(5), 455–461 (2002)
26. W.J. Kim, J.K. Kim, H.K. Kim, J.W. Park, Y.H. Jeong, Effect of post equal-channel-angular-pressing aging on the modified 7075 Al alloy containing Sc. J. Alloys Compd. **450**(1–2), 222–228 (2008)